Compact Transreflective Color Filters and Polarizers by Bilayer Metallic Nanowire Gratings on Flexible Substrates

Zhi-Cheng Ye, Jun Zheng, Shu Sun, Lin-Dong Guo, and Han-Ping D. Shieh, *Fellow, IEEE*

***Abstract*—An integrated transmitted polarizer and reflective color filters with structure of bilayer metallic nanowire grating on a flexible polyethylene terephthalate substrate was demonstrated by theory, experiment, and numerical simulation. Two kinds of waveguide resonances, which led to the comprehensive characters, were analyzed. The slits in the bilayer metallic grating permit the transmission of TM light (transverse magnetic field) in surface plasmon waveguide mode and prohibit the propagating of TE light (transverse electric field) with wavelengths larger than cutoff value to obtain polarization effect. The lateral guiding mode resonances on the interfaces of the metallic/substrate or metallic/air excite surface plasmon waves with certain wavelengths, which makes a single peak in the reflection spectrum of TM light and dips in transmission for color filtering effect of TM light. The experimental results and theoretical analyses are in good agreement. This new bilayer structure featured with nonabsorption, integrated functions and simple fabrication has a great potential in power saving and thickness reduction for display devices.**

***Index Terms*—Color filter, metallic nanowire, polarizer, surface plasmon.**

I. Introduction

SURFACE plasmon, electromagnetic wave resonance at metal surface with free electrons, are attractive due to their enhanced local intensity, small dimensions, and the ability to manipulate photons efficiently, which have been active research topics in sensors [1], light emitting diodes [2], and optical waveguides [3].

In displays, polarizers and color filters are the two key elements [4] in low optical efficiency, due to the fact that the conventional ones are of absorptive, which, respectively, only allows 50% and 33% of the incident light to pass and absorb the rest. In order to reduce the power consumption, reflective devices that permitting specific light to pass and reflecting otherwise absorptive one for recycle were proposed [5], [6]. Among those devices, metallic nanowire gratings are one of the most promising candidates. It is revealed that the polarization function of subwavelength metallic grating (SWMG) owns to the surface plasmon waveguide resonance (SPWR) inside the metal openings [7]. By setting circular or straight gratings near holes or slits in the metal, due to the grating diffraction coupling, the TM transmission is enhanced [8]. When the SWMG is covered with a suitable dielectric, band pass color filtering can be yielded [9]. The plasmonic color filter for CMOS imaging sensor was reported [10]. The incident angle independent reflective color filter has been studied [11] as well. Furthermore, the feasibility of combining the polarizing and filtering functions using just single SWMG was discussed [12] and the fabrication of SWMGs on flexible substrates using nanoimprinting was reported recently [13].

In this study, a new bilayer metallic nanowire grating on a flexible PET substrate was fabricated, measured, and analyzed. The TM transmission is much higher than that of TE light. There are dips in the TM transmission; the reflected TM light has a single peak and most of the TE light is reflected. The optical mechanism of SPWR is revealed. It provides a convenient and effective means of achieving the polarizing and filtering functions simultaneously. The optical device can be made by a simple fabrication processing without the need of lift-off [14] process on a flexible substrate.

II. Basic Theory and Grating Structure

A schematic of the bilayer metallic nanowire grating is plotted in Fig. 1, where the structure parameters are labeled as well. There are two kinds of waveguide resonances in the metallic gratings: 1) The excitation and coupling of longitudinal slit waveguide modes [15] of aluminum-air-aluminum and aluminum-dielectric-aluminum (SWM-Al/Air/Al and SWM-Al/Di/Al in Fig. 1) which permit the transmission of TM light by surface plasmon mode and suppress that of TE light due to the cutoff of guiding mode. 2) The grating induced lateral surface plasmon resonances (SPR) on the aluminum/substrate and aluminum/air interfaces (SPR-Al/Substrate and SPR-Al/Air in Fig. 1) which induce dips in the transmission and peaks in the reflection spectra [16].

The metallic gratings can be fabricated by nanoimprinting [17], electron beam lithography [18], and laser interfere

Manuscript received July 10, 2012; revised September 2, 2012; accepted October 23, 2012. Date of publication November 16, 2012; date of current version April 25, 2013. This work was supported by the National Natural Science Foundation of China under Grant 61007025 and Grant 10905039, and the Ministry of Education under Grant 20100073120034 and Grant 20090073120076.

Z.-C. Ye and L.-D. Guo are with the National Engineering Laboratory for TFT-LCD Technology, Department of Electronic Engineering, Shanghai Jiao Tong University, Shanghai 200240, China (e-mail: yzhch@sjtu.edu.cn; guolindong@sjtu.edu.cn).

J. Zheng and S. Sun are with the Laboratory for Laser Plasmas (Ministry of Education) and the Department of Physics, Shanghai Jiao Tong University, Shanghai 200240, China (e-mail: jzheng@sjtu.edu.cn; xyss0818@126.com).

H.-P. D. Shieh is with the Department of Photonics and the Display Institute, National Chiao Tung University, Hsinchu 300, Taiwan (e-mail: hpshieh@mail.nctu.edu.tw).

Color versions of one or more of the figures in this paper are available online at http://ieeexplore.ieee.org.

Digital Object Identifier 10.1109/JSTQE.2012.2227247

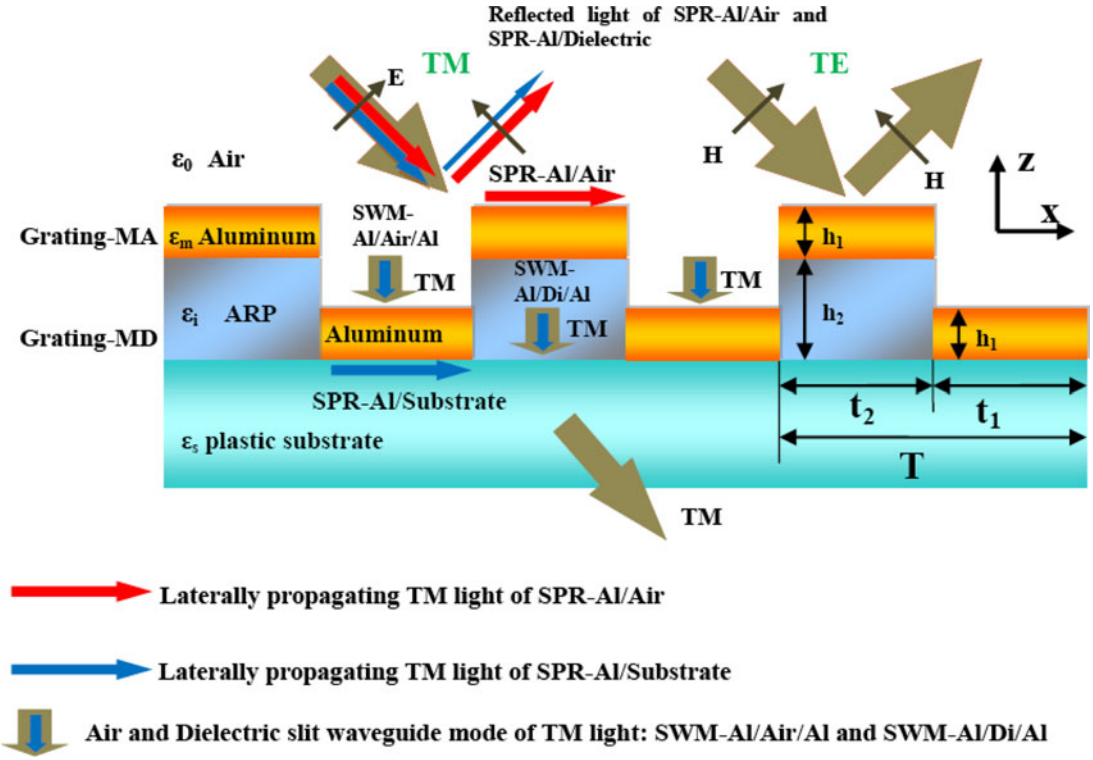

Fig. 1. Schematic of the bilayer metallic nanowire grating and the waveguide resonances therein. Grating-MA: the grating with metal and air. Grating-MD: the grating with metal and dielectric. SPR-Al/Air: the grating-induced lateral surface plasmon resonance on the aluminum/air interface. SPR-Al/Substrate: the grating-induced lateral SPR on the aluminum/substrate interface. SWM-Al/Air/Al: the waveguide modes of the aluminum-air-aluminum slit. SWM-Al/Di/Al: the waveguide modes of the aluminum-dielectric-aluminum slit. The permittivity $\varepsilon_s = 2.25$, $\varepsilon_i = 2.25$, ε_m , and $\varepsilon_0 = 1$ are of plastic substrate, Allresist Photoresist (ARP) dielectric, aluminum, and air, respectively. The height of the aluminum layer $h_1 = 70$ nm, the height of the dielectric layer $h_2 = 150$ nm, the pitch $T = 460$ nm, the width of metal, and dielectric $t_1 = t_2 = $ T/2.

lithography [19]. The laser interference lithography is featured with simple process, high throughput, and low cost. In this study, a dielectric (ARP3500–6, Allresisit GmbH) grating with period $T = 460$ nm and depth h_2 about 150 nm was fabricated by two beam laser interference using a He–Cd laser (442 nm, KIMMON) with a cross angle of 32° on a PET substrate. Then, an aluminum film of thickness $h_1 = 70$ nm was deposited on the grating using E-beam depositor (ei-5z), which cloned the profile of the dielectric grating automatically. Thus, a bilayer metallic grating was obtained. The optical photographs of the sample are shown in Fig. 2(a), where, from left to right, the first three photographs are diffraction under different observation angles with red, yellow, and green color; the fourth was taken by bending the substrate. The scanning electronic microscopy (SEM) image of the top view and the atomic force microscopy (AFM) image of a typical fabricated metallic grating are shown in Fig. 2(b) and (c), respectively. Fig 2(c) reveals that the height difference of the two metallic layers is about 150 nm, which is also the depth of the dielectric grating h_2.

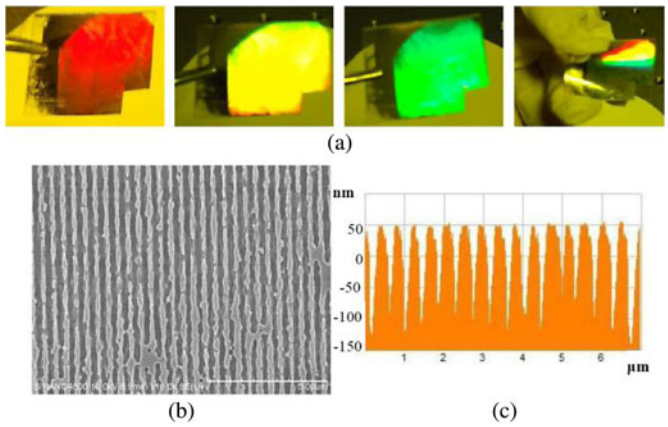

Fig. 2. (a) Optical photographs, (b) SEM, and (c) AFM images of the fabricated bilayer aluminum nanowire grating. For (a), from left to right, the first three photographs are the diffraction under different observation angles with red, yellow, and green color, and the fourth was taken by bending the substrate.

III. Results and Discussion

A. Color Filter Effect

The schematic of the optical measurement is shown in Fig. 3(a), where a collimated white light is filtered by a Glen–Thompson polarizer (CVI–MG) and then is incident upon the nanowire gratings on a PET substrate. The nanowire gratings are rotated at a fixed incident angle. When the grating lines are parallel to the electric field of the incident light, it is TE incidence, while TM incidence for the vertical case. The transmitted and reflected lights are collected by a fiber mounted with a collimated lens to a spectrometer (USB 4000, Ocean Optics) normalized by the incident light. The measured TM transmission spectra for incident angles 0°, 10°, and 20° from the top metal layer are

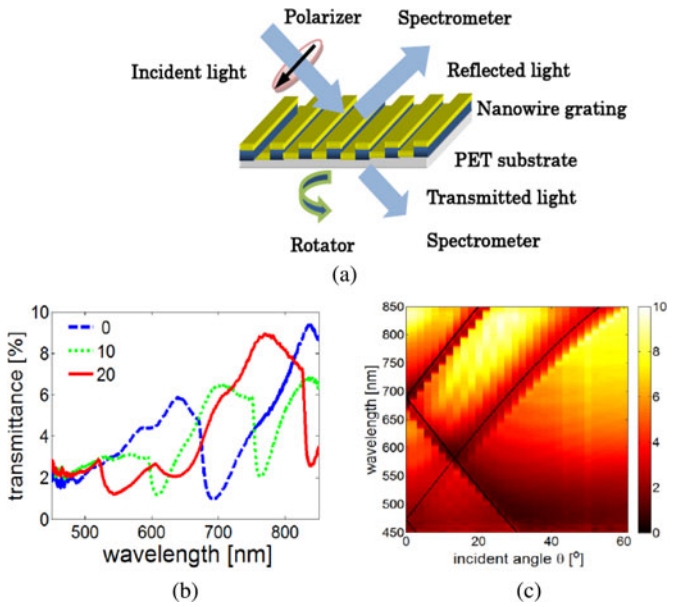

Fig. 3. (a) Schematic of the optical measurement, (b) and (c) transmission of the TM light at different incident angles.

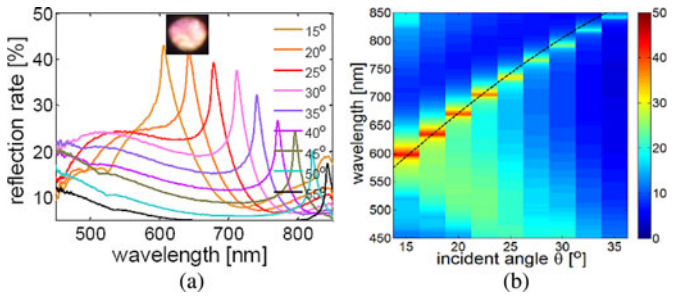

Fig. 4. Reflection of TM by every 5° from 15° to 55°. The inset in Fig. 4(a) is the photo of the reflection with an incident angle of 20°.

shown in Fig. 3(b). In each curve, there is one, two, or three dips, which correspond to the SPR-Al/Air and SPR-Al/Substrate derived by (1) [20]. Fig. 3(c) shows the transmission spectra for every 5° incident angle measured from 0° to 60°, where the three distinct black lines indicating the dips of transmission are the results of the dispersion relationship (1) for SPR on the Al surfaces as aforementioned. It is clear that the data derived by (1) of lateral SPR-Al/Air and SPR-Al/Substrate resonances are in good agreement with the measured dips, implying that the excited lateral surface plasmon modes cannot be transmitted through the bilayer metallic grating, thus the transmission has color filtering effect. Part of the lights propagate along the grating surfaces in lateral SPR-Al/Air and SPR-Al/Substrate and some are reflected back as shown in the measured reflection peaks in Fig. 4. The dashed black line in Fig. 4(b) is corresponding to SPR-Al/Air, the same as the line in Fig. 3(c). The single peaks in the reflection spectra [see Fig. 4(a)] clearly show that the grating can work as a reflective color filter for TM light

$$k_0 \sin\theta + nG = k_0 \sqrt{\frac{\varepsilon_{i/0}\varepsilon_m}{\varepsilon_{i/0} + \varepsilon_m}}. \tag{1}$$

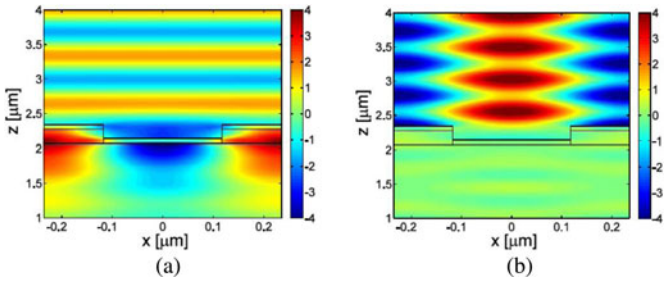

Fig. 5. Obtained magnetic field H_y using Rigorous Coupled Wave Analysis (RSOFT, DiffractMOD) for the SPR-Al/Substrate and SPR-Al/Air, The black lines depict schematically the profile of the bilayer grating. The light is normally incident on the gratings along the minus direction of Z-axis with incident wavelengths: (a) 690 nm and (b) 470 nm.

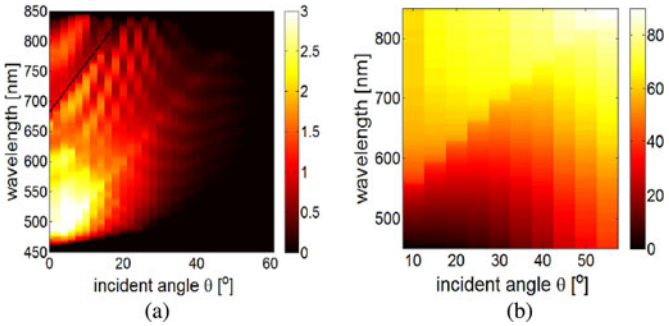

Fig. 6. Transmission (a) and reflection (b) spectra of TE light under incident angles from 0° to 60° by every 5°.

In (1), k_0 is the wave vector of the incident light, θ is the incident angle, $G = 2\pi/T$ is the unit of grating vector, $n = \pm 1$, ± 2, ... is the diffraction order of the grating, $\varepsilon_{i/0}$ and ε_m are the permittivity of the dielectric (ε_i: PET substrate permittivity and ε_0: air permittivity) and aluminum [21]. The solid and dash black lines in Fig. 3(c) are corresponding to SPR-Al/Substrate and SPR-Al/Air by the ± 1 order diffraction, respectively.

To show the SPR modes clearly, the magnetic field profiles H_y calculated by Rigorous Coupled Wave Analysis (RSOFT, DiffractMOD) with the incident angle 0° are given in Fig. 5. The wavelength of the incident light is 690 nm in Fig. 5(a), where SPR-Al/Substrate appears. Fig. 5(b) shows the GSPR-Al/Air with the wavelength of 470 nm. From Fig. 5, we can see that for SPR-Al/Substrate the maximum field intensity is on the interface between aluminum and substrate, while for SPR-Al/Air it is on the interface between aluminum and air. It is consistent with the character of SP polaritons. Moreover, the strong reflections of the light due to the SPR resonances, especially of SPR-Al/Air, are apparently observed form Fig. 5.

B. Polarizer Effect

The measured transmission and reflection spectra of TE light incident from the top are shown in Fig. 6. In Fig. 6(a), the dips highlighted with the black dashed line correspond to the waveguide modes in the substrate, which follows $k_0 \sin\theta + nG \approx k_0\sqrt{\varepsilon_i}$ [22]. The transmission is much lower than the corresponding TM case in Fig. 3(c). Especially for the large incident angles, the TE transmittance is reduced to almost zero, while

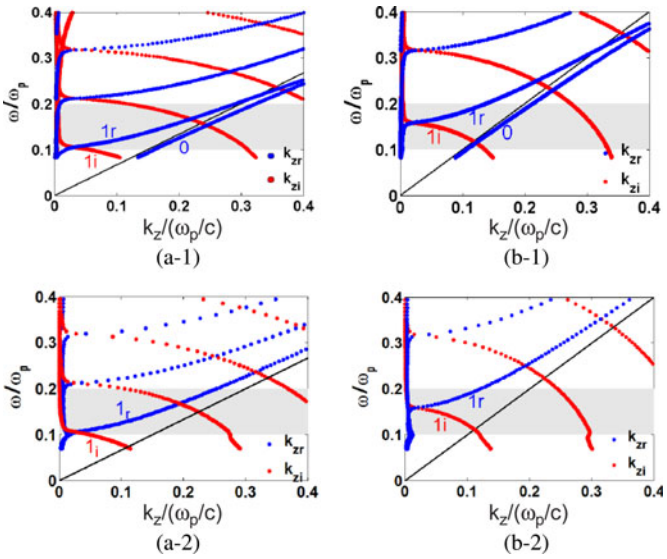

Fig. 7. Dispersion of the slits waveguide modes of the bottom Grating-Al/Substrate (a-1, a-2) and top Grating-Al/Air (b-1, b-2). Figures of (a-1) and (b-1) are for the TM light, and figures (a-2) and (b-2) are for the TE light.

the TM transmittance is even increased. For the incident angle of 60°, the extinction rate of transmitted TM to TE light is as high as 60. While the TE reflection shown in Fig. 6(b) is much higher than the TM reflection in Fig. 4, implying that the nontransmissive TE light is reflected. The no-absorptive polarization effect is demonstrated as well. The different transmission between TM and TE light can be explained as later.

Because of the periodic character, the dispersion of waveguide modes in the slits (SWM) is described by (2) deduced from Bloch theory [23]

$$\cos(KT) = \cos(k_1 t_1)\cos(k_2 t_2) - 1/2(g + 1/g)\sin(k_1 t_1)\sin(k_2 t_2) \quad (2)$$

where K denotes the Bloch wave number, T is the pitch of the grating, t_1 and t_2 are the thickness of the dielectric and aluminum in one period, respectively, $k_1 = k_0^2 \varepsilon_{i/0} - k_z^2$ and $k_2 = k_0^2 \varepsilon_m - k_z^2$ are the wave numbers of the input light in the dielectric and aluminum along the X-axis, respectively. k_z is the wave number of the waveguide mode along the Z-axis. $g = k_1 \varepsilon_m / (k_2 \varepsilon_{i/0})$ for TM light and k_1/k_2 for TE light.

The complex solutions of (2) with the structure parameters in our experiments are shown in Fig. 7. The gray part highlights the visible light zone. The blue and red dots are the real and imaginary parts of the wave number k_z, respectively. The black lines represent the dielectric lines of the slits [dielectric slits in Fig. 7(a) and air slits in Fig. 7(b)].

For TM light, the lines beneath the black dielectric line [lines denoted by 0 in Fig. 7(a-1) and (b-1)] represent surface plasmon waveguide modes with negligible K_{zi}, which are SWM-Al/Air/Al and SWM-Al/Di/Al shown in Fig. 1. For both polarizations, the lines above the dielectric lines (lines denoted by 1r, 1i) are the regular lossy waveguide modes, in which, K_{zi} decreases with the increase of the angular frequency ω; When K_{zi} is comparable with or even larger than K_{zr}, it means the waveguide mode is not supported to propagate (cutoff). Hence, for regular modes, the angular frequency ω corresponding to the point of $k_{\mathrm{zi}} = K_{\mathrm{zr}}$ is called the cutoff frequency and only frequencies above it can be transmitted through the slits. It is noted that the cutoff frequencies of the first-order TE modes equal to the second-order TM mode, which are 0.105 ω_p (788 nm) and 0.162 ω_p (511 nm) for dielectric and air slits, respectively. Thus, the TE light is forbidden to pass for wavelengths larger than 511 nm. While for the surface plasmon waveguide modes [line 0 in Fig. 7(a-1) and (b-1)] of TM light, there is no cutoff frequency, indicating that the TM light can always pass through the slits in surface plasmon waveguide modes.

The previous analyses show that the polarization of the structure originates from the polarization selective transmission of the grating slits. In addition, the reason that the reflection of TE is higher than that of the TM is that TE light cannot enter the silts, thus is reflected back like incident on an aluminum film.

From the measurements and analyses previously, we can see that the structure acts as a color filter and a polarizer simultaneously. The transmission effect can be used as a compact integrated color filter and polarizer, which can be applied for display devices and other imaging sensors. Different from the conventional absorption-type filters or polarizers, the structure studied here does not absorb the light for the realization of the functions of color filtering and polarization. It reflects back the TE light while allowing the passing of TM light. In addition, it reflects back the TM light of SPR-Al/Air to function as a color filter in both transmission and reflection. This peculiar character makes the structure suitable for display application for power saving by recycling the reflected TE or TM light.

IV. Conclusion

Laser interference lithography was employed to fabricate the dielectric reliefs on PET substrates, and then E-beam evaporator was used to deposit aluminum on top of reliefs and inside the slits to obtain bilayer metallic grating. Slit and substrate surface plasmon waveguide modes were investigated analytically and experimentally. For wavelengths larger than cutoff value, the TE light is prohibited and only the TM light is permitted to pass through the slits. Thus, the grating acts as a TM pass polarizer. With the lateral surface plasmon waveguide resonances on the interfaces of aluminum /air, the TM light is reflected back and there is a single peak in reflection and multiple dips in transmission. Both the reflection and transmission spectra have color filtering effect. Different from the conventional absorptive ones, the bilayer metallic nanowire does not absorb the incident light, which has great advantage for power saving in displays. In addition, the structure is compact as an integration film of polarizer and color filter, which can reduce the thickness of the display devices. By optimizing the fabrication process, the proposed metallic nanowire gratings in color filtering and polarization functions can be further improved.

Acknowledgment

Aluminum deposition was carried out in Suzhou Institute of Nanotech and Nanobionics. The AFM and SEM pictures

were measured by Instrumental Analysis Center of Shanghai Jiao Tong University and Suzhou Institute of Nanotech and Nanobionics, respectively.

REFERENCES

[1] O. Limaj, S. Lupi, F. Mattioli, R. Leoni, and M. Ortolani,, "Midinfrared surface plasmon sensor based on a substrateless metal mesh," *Appl. Phys. Lett.*, vol. 98, pp. 091902-1–3, 2011.

[2] K. Okamoto, I. Niki, A. Shvartser, Y. Narukawa, T. Mukai, and A. Scherer,, "Surface plasmon enhanced light-emitters based on InGaN quantum wells," *Nat. Mater.*, vol. 3, pp. 601–605, 2011.

[3] J. A. Dionne, A. Sweatlock, H. A. Atwater, and A. Polman,, "Plasmon slot waveguides: Towards chip-scale propagation with subwavelength-scale localization," *Phy. Rev. B.*, vol. 73, pp. 035407–035416, 2006.

[4] H. Kawamoto,, "The history of liquid-crystal displays," *Proc. IEEE*, vol. 90, pp. 460–500, 2002.

[5] C.-C. Tsai and S.-T. Wu,, "Broadband wide-angle polarization converter for LCD backlight," *Appl. Opt.*, vol. 47, pp. 2882–2887, 2008.

[6] M. F. Weber, C. A. Stover, L. R. Gilbert, T. J. Nevitt, and A. J. Ouderkirk, "Giant birefringent optics in multilayer polymer mirrors," *Science*, vol. 287, no. 5462, pp. 2451–2456, 2000.

[7] Y. Ekinci, H. H. Solak, C. David, and H. Sigg,, "Bilayer Al wire-grids as broadband and high performance polarizers," *Opt. Exp.*, vol. 14, pp. 2323–2334, 2006.

[8] D. M. Koller, A. Hohenau, H. Ditlbacher, N. Galler, F. Reil, F. R. Aussenegg, A. Leitner, E. J. W. List, and J. R. Krenn,, "Organic plasmon-emitting diode," *Nature Photon.*, vol. 2, pp. 684–687, 2008.

[9] H.-S. Lee, Y.-T. Yoon, S.-S. Lee, S.-H. Kim, and K.-D. Lee,, "Color filter based on a subwavelength patterned metal grating," *Opt. Exp*, vol. 15, 15457, 2007.

[10] C. M. Wang, Y. C. Chang, M. W. Tsai, Y. H. Ye, C. Y. Chen, Y. W. Jiang, S. C. Lee, and D. P. Tsai,, "Angular independent infrared filter assisted by localized surface plasmon polariton," *IEEE Photon. Technol. Lett.*, vol. 20, pp. 1103–1105, 2008.

[11] S. Yokogawa, S. P. Burgos, and H. A. Atwater, *Nano Lett.*, vol. 12, p. 4349, 2012.

[12] T. Xu, Y.-K. Wu, X. Luo, and L. Jay Guo, *Nature Commun.*, vol. 1:59, p. 1, 2010.

[13] Z. Yu, P. Deshpande, W. Wu, J. Wang, and S. Y. Chou, *Appl. Phys. Lett.*, vol. 77, p. 927, 2000.

[14] A. Voigt, M. Heinrich, K. Hauck, R. Mientus, G. Gruetzner, M. Töpper, and O. Ehrmann, *Microelectron. Eng.*, vol. 78, p. 503, 2005.

[15] Y. Kanamori, M. Shimono, and K. Hane, *IEEE Photonics Technol. Lett.*, vol. 18, p. 2126, 2006.

[16] A. Szeghalmi, M. Helgert, R. Brunner, F. Heyroth, U. Gösele, and M. Knez, *Adv. Funct. Mater.*, vol. 20, p. 2053, 2010.

[17] L. Chen, J. J. Wang, F. Walters, X. Deng, M. Buonanno, S. Tai, and X. Liu, *Appl. Phys. Lett.*, vol. 90, p. 063111, 2007.

[18] T. Ongarello, F. Romanato, P. Zilio, and M. Massari, *Opt. Exp.*, vol. 19, p. 9426, 2011.

[19] P. B. Catrysse, W. Suh, S. Fan, and M. Peeters, *Opt. Lett.*, vol. 29, p. 974, 2004.

[20] A. V. Zayats, I. I. Smolyaninov, and A. A. Maradudin, *Phys. Rep.*, vol. 408, p. 131, 2005.

[21] E. D. Palik,, *Handbook of Optical Constants of Solids.*. New York: Academic, 1985.

[22] J. H. Song, J. H. Chang, J. Zhang, H. Zhang, M. K. Park, C. Li, and G. Q. Lo,, "Grating Coupler Embedded Silicon Platform for Hybrid Integrated Receivers," *IEEE Photonics Technol. Lett.*, vol. 24, pp. 161–163, 2011.

[23] Z. Ye, J. Zheng, Z. Wang, and D. Liu, *Solid State Commun.*, vol. 136, p. 495, 2005.

Zhi-Cheng Ye was born in 1977. He received the B.S. and Master's degrees from Beijing Normal University, Beijing, China, in 1999 and 2002, respectively, and the Ph.D. degree from the Institute of Semiconductors, Chinese Academy of Sciences, Beijing, China, in 2006.

He is currently an Assistant Professor in the Department of Electronic Engineering, Shanghai Jiao Tong University, Shanghai, China. His research interests include micronano fabrication and nano-optical devices, especially the design and application of nano-optical devices for green displays and lightings.

Jun Zheng was born in 1976. She received the Ph.D. degree in optics from the Institute of Physics, Chinese Academy of Sciences, Beijing, China, in 2006.

From 2006 to 2008, she was a Postdoctoral Fellow in Osaka University. She is currently with the Department of Physics, Shanghai Jiao Tong University, Shanghai, China. Her current research interests include fiber laser, surface plasmon, and laser-plasma interaction.

Shu Sun was born in 1989. She received the B.S. degree from Shanghai Jiao Tong University, Shanghai, China, in 2012.

She is currently with the Laboratory for Laser Plasmas (Ministry of Education) and the Department of Physics Shanghai Jiao Tong University.

Lin-Dong Guo was born in 1989. He received the B.S. degree from Shanghai Jiao Tong University, Shanghai, China, in 2012.

He is currently with the National Engineering Laboratory for TFT-LCD Technology, Department of Electronic Engineering, Shanghai Jiao Tong University.

Han-Ping D. Shieh (S'79–M'86–SM'91–F'08) received the B.S. degree from the National Taiwan University, Taipei, Taiwan, in 1975, and the Ph.D. degree in electrical and computer engineering from Carnegie Mellon University, Pittsburgh, PA, in 1987.

He joined National Chiao Tung University (NCTU), Hsinchu, Taiwan, as a Professor with the Institute of Opto-Electronic Engineering and Microelectronics and Information Research Center (MIRC) in 1992. Prior to this, he was a Research Staff Member with the IBM T.J. Watson Research Center, Yorktown Heights, NY, since 1988. He was an Associate Director with MIRC, NCTU. He founded and served as the Director, Display Institute, NCTU, in 2003, the first such kind of graduate academic institute in the world dedicated for display education and research. He was the Dean, College of Electrical and Computer Engineering, NCTU (2006–2010), and AU Optonics Chair Professor. He has also held an appointment as the Chang Jiang Scholar with Shanghai Jiao Tong University, Shanghai, China, since 2010. His current research interests include display systems, optical MEMS, nano-optical components, and thin-film solar energy.

Dr. Shieh is a Fellow of the Optical Society of America and the Society for Information Display.